



1 **Ice core evidence for decoupling between mid-latitude atmospheric water cycle and Greenland**  
2 **temperature during the last deglaciation**

3 Amaëlle Landais<sup>1,\*</sup>, Emilie Capron<sup>2,3</sup>, Valérie Masson-Delmotte<sup>1</sup>, Samuel Toucanne<sup>4</sup>, Rachael

4 Rhodes<sup>5</sup>, Trevor Popp<sup>2</sup>, Bo Vinther<sup>2</sup>, Bénédicte Minster<sup>1</sup>, Frédéric Prié<sup>1</sup>

5 <sup>1</sup> Laboratoire des Sciences du Climat et de l'Environnement, IPSL, UMR 8212, CEA-CNRS-UVSQ-UPS,  
6 Gif sur Yvette, France

7 <sup>2</sup> Centre for Ice and Climate, Niels Bohr Institute, University of Copenhagen, Juliane Maries Vej 30,  
8 DK-2900, Copenhagen, Denmark;

9 <sup>3</sup> British Antarctic Survey, High Cross, Madingley Road, Cambridge, CB3 0ET, UK

10 <sup>4</sup> IFREMER, Laboratoire Géophysique et enregistrement Sédimentaire, CS 10070, 29280 Plouzané,  
11 France

12 <sup>5</sup> Department of Earth Sciences, University of Cambridge, Downing Street, Cambridge, CB2 3EQ  
13 UK

14

15 \*Corresponding author: phone : +33 (0)169084672, email : [amaelle.landais@lsce.ipsl.fr](mailto:amaelle.landais@lsce.ipsl.fr), ORCID :  
16 0000-0002-5620-5465

17 Keywords: Deglaciation, Water isotopes, <sup>17</sup>O-excess, d-excess, Heinrich event, Mystery interval

18



19 **Abstract**

20 The last deglaciation represents the most recent example of natural global warming associated with  
21 large-scale climate changes. In addition to the long-term global temperature increase, the last  
22 deglaciation onset is punctuated by a sequence of abrupt changes in the Northern Hemisphere. Such  
23 interplay between orbital- and millennial-scale variability is widely documented in paleoclimatic  
24 records but the underlying mechanisms are not fully understood. Limitations arise from the difficulty  
25 in constraining the sequence of events between external forcing, high- and low- latitude climate and  
26 environmental changes.

27 Greenland ice cores provide sub-decadal-scale records across the last deglaciation and contain  
28 fingerprints of climate variations occurring in different regions of the Northern Hemisphere. Here, we  
29 combine new ice d-excess and  $^{17}\text{O}$ -excess records, tracing changes in the mid-latitudes, with ice  $\delta^{18}\text{O}$   
30 records of polar climate. Within Heinrich Stadial 1, we demonstrate a decoupling between climatic  
31 conditions in Greenland and those of the lower latitudes. While Greenland temperature remains  
32 mostly stable from 17.5 to 14.7 ka, significant change in the mid latitudes of northern Atlantic takes  
33 place at  $\sim 16.2$  ka, associated with warmer and wetter conditions of Greenland moisture sources. We  
34 show that this climate modification is coincident with abrupt changes in atmospheric  $\text{CO}_2$  and  $\text{CH}_4$   
35 concentrations recorded in an Antarctic ice core. Our coherent ice core chronological framework and  
36 comparison with other paleoclimate records suggests a mechanism involving two-step freshwater  
37 fluxes in the North Atlantic associated with a southward shift of the intertropical convergence zone.



38

39 **Introduction**

40 The last deglaciation (~19 thousand to 11 thousand years before present, ka) is the most recent major  
41 reorganization of global climate and is thus extensively documented by proxy records from natural  
42 climate archives. The wealth of high-resolution records from well-dated archives and data synthesis  
43 obtained over the past decades show two modes of climate variability during this period (e.g. Denton  
44 et al., 2010, Clark et al., 2012). The first is a long-term increase in global surface temperature and  
45 atmospheric CO<sub>2</sub> concentration between 18 and 11 ka. Superimposed on this is a sequence of  
46 centennial-scale transitions between three quasi-stable intervals documented in Northern  
47 Hemisphere temperature, namely (i) the Heinrich Stadial 1 (~17.5-14.7 ka), that encompasses the  
48 massive rafting episode known as Heinrich event 1 (from ~16 ka); (ii) the Bølling-Allerød warming phase  
49 (~14.7 to 12.9 ka) and (iii) the Younger Dryas cold phase (~12.9 to 11.7 ka). This three-step sequence  
50 coincides with rapid variations in the Atlantic Meridional Oceanic Circulation (AMOC) (Mc Manus et  
51 al., 2004), with evidence for a weak meridional overturning in the North Atlantic during the cold period  
52 encompassing Heinrich Stadial 1 and the Younger Dryas.

53 Our understanding of the mechanisms at play during these North Atlantic cold phases remains limited.  
54 First, recent studies challenge the earlier attribution of the AMOC slowdown during Heinrich Stadial 1  
55 to the impact of the Iceberg Rafted Debris (IRD) from the Laurentide ice sheet through Hudson Strait  
56 (Alvarez-Solas et al., 2011). In particular, meltwater releases from the European ice sheet occurring as  
57 early as 19 or 20 ka may have played an important role in this AMOC slowdown (Toucanne et al., 2010;  
58 Stanford et al., 2011; Hodell et al., 2017).

59 Second, major global reorganizations of the hydrological cycle have been demonstrated during  
60 Heinrich Stadial 1. They can be separated in two phases. In North America, a first time interval  
61 characterized by low lake levels (referred to as the “big dry”, 17.5 to 16.1 ka) was followed by a second  
62 time interval with high lake levels (referred to as the “big wet”, 16.1 to 14.7 ka) (Broecker et al., 2012),



63 both apparently occurring during a stable cold phase in Greenland temperature. The second phase of  
64 Heinrich Stadial 1 is also associated with a weak East Asian monsoon interval (Zhang et al., 2014),  
65 understood to reflect a southward shift of the Inter-tropical Convergence Zone (ITCZ). While there is  
66 growing evidence for large-scale reorganizations of climate and low- to mid- latitude atmospheric  
67 water cycle within Heinrich Stadial 1, the exact sequence of events is not known with sufficient  
68 accuracy to understand the links between changes in North Atlantic climate, AMOC, and the lower  
69 latitude water cycle.

70 Linking changes in the high latitudes of the North Atlantic and the mid- to low- latitudes requires  
71 precise absolute chronologies such as those obtained from annual layer counting of Greenland ice (e.g.  
72 Andersen et al., 2006) or U/Th dating of speleothems (e.g. Zhang et al., 2014). Unfortunately, absolute  
73 dating uncertainties increase above a hundred years during the last deglaciation, precluding a direct  
74 comparison of proxy records at the centennial scale. In this study, we circumvent this difficulty by using  
75 a diverse range of proxy records measured on Greenland ice cores that represent both Greenland  
76 temperature and mid-latitude moisture source conditions.

#### 77 **Analytical method**

78 Here, we present new water isotope records ( $\delta^{18}\text{O}$ , d-excess,  $^{17}\text{O}$ -excess) from the NGRIP ice core  
79 (NGRIP et al., 2004), reported on the annual-layer counted Greenland Ice Core Chronology 2005  
80 (hereafter GICC05, Rasmussen et al., 2006; Svensson et al., 2008), and associated with relatively small  
81 absolute uncertainties over the last deglaciation (maximum counting  $1\sigma$  error of 100-200 yr). Other  
82 Greenland and Antarctic ice cores have been aligned on the GICC05 chronology, with a maximum  
83 relative dating uncertainty of 400 years over the last deglaciation (Rasmussen et al., 2008; Bazin et al.  
84 2013; Veres et al., 2013).

85 The new NGRIP  $\delta^{18}\text{O}$  and  $\delta\text{D}$  dataset was obtained at Laboratoire des Sciences du Climat et de  
86 l'Environnement (LSCE) using a laser cavity ring-down spectroscopy (CRDS) analyzer PICARRO. The  
87 accuracy for  $\delta^{18}\text{O}$  and  $\delta\text{D}$  measurements displayed here is about 0.1‰ and 1‰ respectively. This new



88 dataset completes the NGRIP high-resolution isotopic dataset published over the time period 11.5 to  
89 14.7 ka with  $\delta^{18}\text{O}$  and  $\delta\text{D}$  measured respectively at the University of Copenhagen and at the Institute  
90 of Arctic and Alpine Research (INSTAAR) Stable Isotope Lab (SIL) (University of Colorado), respectively.  
91  $\delta^{18}\text{O}$  analyses were performed at the Niels Bohr Institute (University of Copenhagen) using a  $\text{CO}_2$   
92 equilibration technique (Epstein et al., 1953) with an analytical precision of 0.07‰.  $\delta\text{D}$  measurements  
93 at INSTAAR were made via an automated uranium reduction system coupled to a VG SIRA II dual inlet  
94 mass spectrometer (Vaughn et al., 1998). Analytical precision for  $\delta\text{D}$  is  $\pm 0.5\text{‰}$  or better. Both series  
95 show similar  $\delta^{18}\text{O}$  values, in agreement with the reference  $\delta^{18}\text{O}$  series for NGRIP over the last climatic  
96 cycle (NGRIP community members, 2004) within error bars. However, while both LSCE and INSTAAR  
97 SIL d-excess series display the same 3.5‰ decrease over the onset of Bølling-Allerød, the mean d-  
98 excess level differs by 2.5‰ between the two timeseries. Despite several home standard  
99 intercalibrations between the two laboratories, this difference remains unexplained and prevents any  
100 further discussion on the absolute NGRIP d-excess levels. The new and published NGRIP d-excess  
101 dataset are combined after a shift of the INSTAR SIL d-excess series by -2.5‰.

102 In order to perform  $^{17}\text{O}$ -excess measurements on water samples at LSCE, water reacts with  $\text{CoF}_3$  to  
103 produce oxygen whose triple isotopic composition is measured by dual inlet against a reference  $\text{O}_2$  gas  
104 resulting in a mean uncertainty of 5 ppm (1  $\sigma$ ) for the  $^{17}\text{O}$ -excess measurements (Barkan and Luz,  
105 2005). Every day, at least one home standard is run with the batch of samples to check the stability of  
106 the fluorination line and mass spectrometer and a series of water home standards whose  $\delta^{18}\text{O}$   
107 encompasses the SMOW – SLAP scale is run every month enabling to calibrate the  $\delta^{18}\text{O}$  and  $^{17}\text{O}$ -excess  
108 values (Schoenemann et al., 2013).

## 109 **Results**

110 Ice core  $\delta^{18}\text{O}$  (NGRIP community members, 2004) is a qualitative proxy for local surface temperature.  
111 Comparisons between ice core  $\delta^{18}\text{O}$  data and paleotemperature estimates from borehole temperature  
112 profile inversion and abrupt temperature changes inferred from isotopic measurements on trapped



113 air showed that the  $\delta^{18}\text{O}$ -temperature relationship at NGRIP varies from 0.3 to 0.5 ‰ $^{\circ}\text{C}^{-1}$  during  
114 glacial-interglacial periods (Buizert et al., 2014; Dahl-Jensen et al., 1998; Kindler et al., 2014). In  
115 addition to  $\delta^{18}\text{O}$  records already available (NGRIP community members, 2004), we provide here new  
116 d-excess data from NGRIP during the last deglaciation. The second-order parameter d-excess ( $\delta\text{D}-$   
117  $8\times\delta^{18}\text{O}$ ) (Dansgaard, 1964) is used in Greenland ice cores to track past changes in evaporation  
118 conditions or shifts in moisture sources (Johnsen et al., 1989; Masson-Delmotte et al., 2005a).  
119 Evaporation conditions affect the initial vapor d-excess through the impact of surface humidity and  
120 sea surface temperature on kinetic fractionation (Jouzel et al., 1982). Recent vapour monitoring and  
121 modelling studies show that the d-excess signal of the moisture source can be preserved in polar  
122 vapour and precipitation after transportation towards polar regions (Bonne et al., 2015; Pfahl and  
123 Sodemann, 2014). This signal can however be altered during distillation due to the sensitivity of  
124 equilibrium fractionation coefficients to temperature, leading to alternative definitions using  
125 logarithm formulations for Antarctic ice cores (Uemura et al., 2012; Markle et al., 2016). Finally,  
126 changes in  $\delta^{18}\text{O}_{\text{sea water}}$  also influence  $\delta^{18}\text{O}$  and d-excess in polar precipitation. Summarizing, d-excess in  
127 Greenland ice core is a complex tracer: interpreting its past variations in terms of changes in  
128 evaporation conditions (sea surface temperature or humidity) requires deconvolution of the effects of  
129 glacial-interglacial changes in  $\delta^{18}\text{O}_{\text{sea water}}$  and condensation temperature.

130 Our dataset also encompasses new  $^{17}\text{O}$ -excess data from NGRIP. Defined as  $\ln(\delta^{17}\text{O}+1)-$   
131  $0.528*\ln(\delta^{18}\text{O}+1)$ ,  $^{17}\text{O}$ -excess provides complementary information to d-excess (Landais et al., 2008;  
132 Landais et al., 2012). At evaporation, d-excess and  $^{17}\text{O}$ -excess are both primarily influenced by the  
133 balance between kinetic and equilibrium fractionation, itself driven by relative humidity at the sea  
134 surface. During transport, while d-excess is influenced by distillation effects during atmospheric  
135 cooling,  $^{17}\text{O}$ -excess is largely insensitive to this effect, except at very low temperatures in Antarctica  
136 (Winkler et al., 2012). Conversely,  $^{17}\text{O}$ -excess is affected by recycling or mixing of air masses along the  
137 transport path from low to high latitudes (Risi et al., 2010), and by the range over which supersaturated  
138 conditions occur, itself affected for instance by changes in sea-ice extent or temperature along the



139 transport path (Schoenemann et al., 2014). Because of its logarithmic definition,  $^{17}\text{O}$ -excess is not  
140 sensitive to changes in  $\delta^{18}\text{O}_{\text{sea water}}$  given that the  $^{17}\text{O}$ -excess of global sea water remains constant with  
141 time.

142 Our 1518 new measurements of  $\delta^{18}\text{O}$  and d-excess on the NGRIP ice core cover the time period 14.5  
143 to 60 ka (Figure 1) and we present 454 duplicate measurements of  $^{17}\text{O}$ -excess over the time period  
144 ranging from 9.6 to 20 ka (Figure 2) (see methods for details). As previously reported for the central  
145 Greenland GRIP ice core (Masson-Delmotte et al., 2005b; Jouzel et al., 2005), the NGRIP  $\delta^{18}\text{O}$  and d-  
146 excess records exhibit a systematic anti-correlation during the abrupt Dansgaard-Oeschger (DO) events  
147 of the last glacial period and last deglaciation (Bølling-Allerød and Younger Dryas), with d-excess being  
148 higher during cool Greenland Stadials and lower during warm Greenland Interstadials.

149 The origin of moisture may be different at GRIP and NGRIP. While both sites are expected to receive  
150 most of their moisture from the North Atlantic (30°N to 55°N, Landais et al., 2012) with modulation  
151 partly linked to sea ice extent (Rhines et al., 2014), the northwestern NGRIP site may also receive  
152 moisture from North Pacific (Langen and Vinther, 2009). Nevertheless, the two sites depict similar  
153 amplitudes of d-excess variations across DO events (Figure 1). We note that this contrasts with a  
154 slightly lower amplitude (typically by 1‰) of abrupt  $\delta^{18}\text{O}$  changes at NGRIP compared to GRIP.

155 The fact that d-excess increases (by  $3.5 \pm 1$  ‰) when  $\delta^{18}\text{O}$  decreases (by  $4 \pm 1$  ‰) during Greenland  
156 stadials relative to interstadials may at least partly reflects the influence of local temperature changes  
157 on d-excess, challenging a simple interpretation in terms of changes in source conditions. We note one  
158 exception, the Heinrich Stadial 1 cold phase preceding the onset of the Bølling-Allerød at 14.7 ka. In  
159 this case,  $\delta^{18}\text{O}$  remains almost stable from 17.5 to 14.7 ka on the three Greenland ice cores NGRIP,  
160 GRIP and GISP2 displayed on Figure 2. Over this period,  $\delta^{18}\text{O}$  variations are smaller than 1 ‰, i.e. less  
161 than one fourth of the average amplitude in  $\delta^{18}\text{O}$  changes across DO events, suggesting no large  
162 temperature change in Greenland during this period. The link between flat  $\delta^{18}\text{O}$  and minimal  
163 temperature variability can be challenged since a mean temperature signal can be masked by a change



164 in seasonality of moisture source origin on the  $\delta^{18}\text{O}$  record (Boyle et al., 1994; Krinner et al., 1997).  
165 However, our assumption of stable temperature is supported by constant  $\delta^{15}\text{N}$  of  $\text{N}_2$  values in the GISP2  
166 and NGRIP ice cores (Buizert et al., 2014),  $\delta^{15}\text{N}$  of  $\text{N}_2$  being an alternative paleothermometry tool in ice  
167 core that is not affected by processes within the water cycle (Severinghaus and Brook, 1999). In  
168 contrast to this almost stable  $\delta^{18}\text{O}$  signal, d-excess depicts an average 2.2 ‰ increase at 16.1 ka (more  
169 than 60% of the average amplitude during DO events) with a larger amplitude at GRIP (2.7 ‰) than at  
170 NGRIP (1.7 ‰) (Figure 2). In this case, the increase in d-excess cannot be explained by any Greenland  
171 temperature change, and therefore demonstrates a decoupling between cold and stable Greenland  
172 temperatures and changing climatic conditions at lower latitudes during Heinrich Stadial 1 (see also  
173 SOM).

174 While the  $^{17}\text{O}$ -excess level is similar at the Last Glacial Maximum (i.e. before 19 ka on Figure 2) and the  
175 Early Holocene (40 ppm), it also shows significant variations during the last deglaciation. Most of these  
176 variations co-vary with those of  $\delta^{18}\text{O}$  such as the four main oscillations during the Bølling-Allerød and  
177 the onset and end of the Younger Dryas. They can be interpreted as parallel variations in the Greenland  
178 temperature and lower latitude climate with a possible contribution of local temperature through  
179 kinetic effects. Again, a major difference occurs during Heinrich Stadial 1. While the  $\delta^{18}\text{O}$  record is  
180 relatively stable,  $^{17}\text{O}$ -excess exhibits a decreasing trend (strongest between 17.5 and 16.1 ka) before a  
181 minimum level is reached between 16.1 to 14.7 ka. We therefore observe a clear and synchronous  
182 signal in both d-excess and  $^{17}\text{O}$ -excess dated around 16.2 ka from statistical analysis (cf. section  
183 statistical analyses in SOM). These  $^{17}\text{O}$ -excess and d-excess transitions at 16.2 ka do not have any clear  
184 counterpart in  $\delta^{18}\text{O}$  (cf section correlation in SOM) and no temperature variation at that time was  
185 recorded in the  $\delta^{15}\text{N}$  of  $\text{N}_2$  record. We interpret these patterns as illustrating a reorganization of  
186 climatic conditions and/or water cycle at latitudes south of Greenland. A similar shift in  $^{17}\text{O}$ -excess has  
187 already been observed during Heinrich Stadial 4 in the NEEM ice core, while the  $\delta^{18}\text{O}$  record exhibits a  
188 constant low level (Guillevic et al., 2014). This pattern was also attributed to a change in the water  
189 cycle and/or climate at lower latitudes.



190 **Discussion**

191 The Greenland water stable isotope records demonstrate a change in the water cycle and/or climate  
192 at lower latitudes at 16.2 ka when Greenland conditions were relatively stable and cold. This change  
193 at low latitudes is confirmed by the high resolution atmospheric CH<sub>4</sub> concentration record from the  
194 WAIS Divide ice core (Rhodes et al., 2015), presented on the same timescale (Figure 2). At 16.2 ka, the  
195 CH<sub>4</sub> record indeed exhibits a 30 ppbv peak understood to reflect more CH<sub>4</sub> production in Southern  
196 Hemisphere wetlands, driven by wetter conditions due to a southward shift of the tropical rainbelts  
197 associated with the ITCZ (Rhodes et al., 2015). The parallel increase of atmospheric CO<sub>2</sub> concentration  
198 by 10 ppm in ~100 years (Marcott et al., 2013) is understood to result from increased terrestrial carbon  
199 fluxes or enhanced air-sea gas exchange in the Southern Ocean (Bauska et al., 2014). We also highlight  
200 an unusual characteristic of the bipolar seesaw pattern in Antarctic ice core δ<sup>18</sup>O records at 16.2 ka. As  
201 observed during all Greenland Stadials of the last glacial period, Antarctic δ<sup>18</sup>O also increases during  
202 Heinrich Stadial 1 (e.g. EPICA community members, 2006), through the warming phase of Antarctic  
203 Isotopic Maximum 1. The EPICA Dronning Maud Land (EDML) ice core, drilled in the Atlantic sector of  
204 Antarctica, shows an associated two step δ<sup>18</sup>O increase. The first step, marked by a strong increasing  
205 trend, is followed by a change in slope at 16.2 ka. The second step is characterized by a slower  
206 increasing trend from 16.2 to 14.7 ka (EPICA community members, 2006; Stenni et al., 2011) (Figure  
207 2). The EDML δ<sup>18</sup>O variations are expected to be closely connected to changes in AMOC due to the  
208 position of the ice core site on the Atlantic sector of the East Antarctic plateau. For other Antarctic  
209 sites, the change of slope around 16.2 ka is less clear, probably due to the damping effect of the  
210 Southern Ocean or because other climatic effects linked to atmospheric teleconnections with the  
211 tropics affect the Pacific and Indian sectors of Antarctica (Stenni et al., 2011, WAIS Divide members,  
212 2013 Buiron et al., 2012). A change in the teleconnections between West Antarctic climate and tropical  
213 regions is also observed around 16.2 ka (Jones et al., 2018). Summarizing, our synthesis of ice core  
214 records clearly demonstrates a climate shift at 16.2 ka, identified in proxy records sensitive to shifts in  
215 tropical hydrology (CH<sub>4</sub>), mid-latitude hydrological cycle changes in the Atlantic basin (Greenland



216 second order isotopic tracers), as well as in Antarctic climate dynamics in the Atlantic basin. This  
217 suggests some reorganization of water cycle in the Atlantic region (possibly involving AMOC) related  
218 to surface shifts in the ITCZ at 16.2 ka. This does not appear to affect the high latitudes of the North  
219 Atlantic as Greenland temperatures stay uniformly cold.

220 At low latitudes, an ITCZ shift at 16.2 ka is clearly expressed through a weak monsoon interval in East  
221 Asian speleothem records and through change in hydrology in the low-latitude Pacific region and Brazil  
222 (Partin et al., 2007; Russell et al., 2014; Strikis et al., 2015). Since we have ruled out a local temperature  
223 signal at 16.2 ka in Greenland, the origin of the Greenland  $\delta$ -excess and  $^{17}\text{O}$ -excess changes around  
224 16.2 ka is also linked to changes in the climate of the source evaporative regions. When evaporation  
225 conditions change, they affect the proportion of kinetic versus equilibrium fractionation, and cause  
226 similar trends in both  $\delta$ -excess and  $^{17}\text{O}$ -excess. Both of them indeed increase when kinetic fractionation  
227 is more important, i.e. when relative humidity decreases, or when a change in sea ice modifies the  
228 evaporative conditions (Klein et al., 2015; Kopec et al., 2016). However,  $\delta$ -excess in the atmospheric  
229 vapor is affected by distillation toward higher latitudes, and strongly depends on the source-site  
230 temperature gradient, while  $^{17}\text{O}$ -excess preserves better the initial fingerprint of relative humidity of  
231 the evaporative region.

232 As a result, the opposing trends observed in  $\delta$ -excess and  $^{17}\text{O}$ -excess at 16.2 ka can most probably be  
233 explained by an increase of both the relative humidity and the sea surface temperature of the  
234 evaporative source regions for Central and North Greenland. Despite known limitations (Winkler et al.,  
235 2012, Schoenemann and Steig, 2016), the classical approach for inferring changes in source relative  
236 humidity and surface temperature from  $\delta$ -excess and  $^{17}\text{O}$ -excess in Greenland (Masson-Delmotte et  
237 al., 2005a; Landais et al., 2012) suggests respective increases of the order of 3°C and 8% for  
238 temperature and relative humidity of the source evaporative regions respectively. The larger  $\delta$ -excess  
239 increase at the transition between Phase 1 and Phase 2 of Heinrich Stadial 1 observed at GRIP  
240 compared to NGRIP is compatible with a larger proportion of GRIP moisture provided by the mid-



241 latitude North Atlantic for this site. A larger increase in the sea surface temperature of the source of  
242 moisture for GRIP compared to NGRIP would also reduce the source-site temperature gradient and is  
243 fully compatible with the 2 ‰ less depleted level of  $\delta^{18}\text{O}$  at GRIP, compared to NGRIP, during Phase 2.  
244 The increases in both temperature and relative humidity of the Greenland source regions suggest a  
245 more intense evaporative flux from lower latitudes starting at 16.2 ka. Such features could be  
246 explained either by a local climate signal of evaporative regions or by a southward shift of evaporative  
247 source regions toward warmer and more humid locations. This latter interpretation is in line with  
248 earlier interpretations of Greenland d-excess changes (Steffensen et al., 2018; Masson-Delmotte et al.,  
249 2005b). The Greenland signals may also be at least partly explained by wetter conditions in the  
250 continental North America evaporative source regions, which are known to partly affect Greenland  
251 moisture today in addition to the main source in Northern Atlantic [38]. This relative humidity signal  
252 reconstructed from Greenland  $^{17}\text{O}$ -excess at the transition between Phase 1 and Phase 2 of Heinrich  
253 Stadial 1 coincides with the onset of the “big wet” period in North American records (Broecker and  
254 Putnam, 2012).

255 We now explore paleoceanographic records to search for a fingerprint of climate and/or AMOC  
256 reorganization at 16.2 ka in the North Atlantic region and possible implications for our ice core records.  
257 Such comparison of ice core and marine sediment records appears insightful despite existing  
258 limitations attached to relative chronologies. First, high resolution proxy records of surface sea  
259 temperature in the East Atlantic, near Europe, depict a clear warming in the middle of Heinrich Stadial  
260 1 (Bard et al., 2000; Matrat et al., 2014, Figure 3). This signal is coherent with our interpretation of  
261 Greenland d-excess increase at 16.2 ka. In the deep Western Atlantic, no specific feature emerges  
262 between Phase 1 and Phase 2 of Heinrich Stadial 1 from the multi-centennial resolution record of  
263 Pa/Th, a proxy of AMOC strength (McManus et al., 2004). By contrast, a Pa/Th record from the Iberian  
264 margin (Gerhardi et al., 2005) at shallower depth (1500 m shallower than the western Atlantic record)  
265 shows a significant increase at 16.2 ka. These records may be interpreted as follows. A first



266 modification of the glacial oceanic ventilation occurs at deep depth as early as 18 ka. At 16.2 ka, AMOC  
267 may be further destabilized to additionally affect Pa/Th at shallower depths.

268 Heinrich Stadial 1 is associated with at least two major Iceberg Rafted Debris (IRD) discharges first  
269 identified near the Iberian margin (Bard et al., 2000). They may reflect either the impact of changes in  
270 ocean conditions on ice shelf and ice sheet stabilities (Alvarez-Solas et al., 2011). Alternatively, the  
271 iceberg discharges themselves may have affected the AMOC, which is known to have major impacts  
272 on patterns of sea surface temperature, sea ice, atmospheric circulation, and climate over surrounding  
273 continents. The first IRD phase originated from ice sheet discharges from Northern Europe and Iceland,  
274 causing strong reorganizations in deep circulation of the North East Atlantic (Stanford et al., 2011,  
275 Grousset et al., 2001; Peck et al., 2006) while the second IRD phase is caused by discharges from the  
276 Laurentide ice sheet. Recent studies (e.g. Hodell et al., 2017, Toucanne et al., 2015) suggest that all IRD  
277 phases occur after 16.2 ka, during Heinrich Stadial 1 Phase 2. Before that, Heinrich Stadial Phase 1 is  
278 associated with a strong increase of sediment fluxes due to meltwater arrival through terrestrial  
279 terminating ice streams originating from both European and American sides of the North Atlantic as a  
280 response to the beginning of the deglaciation (Toucanne et al., 2015, Ullman et al., 2015, Leng et al.,  
281 2018) (Figure 3). During the first slowdown of AMOC during Phase 1 of Heinrich Stadial 1, the  
282 associated warming of subsurface water would hence enable the destabilization of marine ice-shelves  
283 occurring during Phase 2 (Alvarez-Solas et al., 2011). This second phase of Heinrich Stadial 1 is also  
284 associated with an extensive sea ice production, south of Greenland (Hillaire-Marcel and De Vernal,  
285 2008). The increase of North Atlantic sea ice extent and major iceberg discharges during the second  
286 phase of Heinrich Stadial 1 are coherent with a southward shift of the evaporative region providing  
287 moisture to Greenland supported by  $\delta$ -excess data, and a southward shift of tropical rainbelts (Chiang  
288 and Bitz, 2005), affecting southern hemisphere  $\text{CH}_4$  sources (Rhodes et al., 2015).

289 **Conclusions**



290 Combined measurements of d-excess and  $^{17}\text{O}$ -excess along the NGRIP ice core demonstrate a  
291 decoupling between a cold and stable Greenland climate and changes in hydroclimate at lower  
292 latitudes during the Heinrich Stadial 1, also referred to as the “Mystery Interval” (Denton et al., 2006).  
293 While Greenland temperature remains mostly stable from 20 to 14.7 ka, a large-scale climatic  
294 reorganization takes place at 16.2 ka, associated with warmer and wetter conditions at the location of  
295 Greenland moisture sources. Based on a coherent temporal framework linking the different ice core  
296 records, we show that this event coincides with changes in the characteristics of the bipolar seesaw  
297 pattern as observed in the Atlantic sector of Antarctica, and has a fingerprint in global atmospheric  
298 composition through sharp changes in atmospheric  $\text{CO}_2$  and  $\text{CH}_4$  concentrations.

299 Based on these new ice core records, their coherent chronology, and the comparison with marine and  
300 terrestrial records, we propose the following sequence of events during the last deglaciation. First, the  
301 initiation of Heinrich Stadial 1 occurs at 17.5 ka or earlier, with meltwater arrival from the terrestrial  
302 terminating ice-streams synchronous with a decrease in the North Atlantic sea surface temperature  
303 off-shore Europe, a first AMOC slowdown, drier conditions in North America, and an increase in  
304 Antarctic temperature as well as in atmospheric  $\text{CO}_2$  and  $\text{CH}_4$  concentrations. No fingerprint of this first  
305 phase of Heinrich Stadial 1 is identified in Greenland water stable isotope records:  $\delta^{18}\text{O}$  (and thus local  
306 temperature),  $^{17}\text{O}$ -excess and d-excess remain stable. A possible explanation for such stability is that  
307 the high-latitude warming induced by the increase in the summer insolation at high latitude over the  
308 beginning of the deglaciation is counterbalanced in Greenland by regional changes in e.g. increased  
309 albedo due to sea ice extent or reduced transport of heat by the atmospheric circulation towards  
310 central Greenland, which both can result from a reduced AMOC strength. The global event occurring  
311 at 16.2 ka marks the onset of the second phase of Heinrich Stadial 1. It is associated with (i) strong  
312 iceberg discharges due to dynamical instability of the Laurentide ice sheet, probably induced by the  
313 accumulation of subsurface ocean heat due to a slowdown of AMOC during Phase 1, (ii) a widespread  
314 reorganization of the atmospheric water cycle in the Atlantic region, with significant changes in d-  
315 excess and  $^{17}\text{O}$ -excess in Greenland, as well as (iii) the initiation of weak monsoon interval in East Asia



316 and (iv) the transition from a “big dry” episode to a “big wet” episodes in North America. We note that  
317 this sequence of events within Heinrich Stadial 1 is invisible in all available Greenland temperature  
318 proxy records, which only display an abrupt warming at the onset of the Bølling-Allerød (14.7 ka).

319 Attached to a bipolar synchronised chronological framework, our new ice core data provide a unique  
320 benchmark to test the ability of Earth system models to correctly resolve the sub-millennial  
321 mechanisms at play during the last deglaciation, and especially the relationships between meltwater  
322 fluxes, the state of the North Atlantic ocean circulation, the Laurentide ice sheet instability, changes at  
323 the moisture sources of Greenland ice cores, the response of hydroclimate at low and high latitudes,  
324 as well as the net quantitative effects on global methane and carbon budgets.

#### 325 **Acknowledgements**

326 The research leading to these results has received funding from the European Research Council  
327 under the European Union’s Seventh Framework Programme (FP7/2007-2013) / RC agreement  
328 number 306045. E. C. is funded by the European Union's Seventh Framework Programme for  
329 research and innovation under the Marie Skłodowska-Curie grant agreement no 600207. R.H.R.  
330 received funding from a European Commission Horizon 2020 Marie Skłodowska-Curie Individual  
331 Fellowship (no. 658120, SEADOG).

332

#### 333 **References**

334 Álvarez-Solas, J., Montoya, M., Ritz, C., Ramstein, G., Charbit, S., Dumas, C., Nisancioglu, K., Dokken,  
335 T. and Ganopolski, A.: Heinrich event 1: an example of dynamical ice-sheet reaction to oceanic  
336 changes, *Clim. Past*, 7(4), 1297–1306, 2011

337 Andersen, K.K., Svensson, A., Johnsen, S.J., Rasmussen, S.O., Bigler, M., Roethlisberger, R., Ruth, U.,  
338 Siggaard-Andersen, M.L., Steffensen, J.P., Dahl-Jensen, D., Vinther, B.M. and Clausen, H.B., The  
339 Greenland Ice Core Chronology 2005, 15–42 ka. Part 1: constructing the time scale, *Quat. Sci. Rev.*,  
340 25(23–24), 3246–3257, 2006

341 Bard, E., Rostek, F., Turon, J.L. and Gendreau, S.: Hydrological Impact of Heinrich Events in the  
342 Subtropical Northeast Atlantic *Science*, 289, 1321–1324, 2000

343 Barkan, E. and Luz, B.: High precision measurements of  $^{17}\text{O}/^{16}\text{O}$  and  $^{18}\text{O}/^{16}\text{O}$  ratios in  $\text{H}_2\text{O}$ , *Rapid*  
344 *Commun., Mass Spectrom.*, 19(24), 3737–3742, 2005



- 345 Bauska, T.K., Baggenstos, D., Brook, E.J., Mix, A.C., Marcott, S. A. and Petrenko, V., Carbon isotopes  
346 characterize rapid changes in atmospheric carbon dioxide during the last deglaciation, *PNAS*, 113(13),  
347 3465-3470, 2016
- 348 Bazin, L., Landais, A., Lemieux-Dudon, B., Toyé Mahamadou Kele, H., Veres, D., Parrenin, P.  
349 Martinerie, P., Ritz, C., Capron, E., Lipenkov, V., Loutre, M.F., Raynaud, D., Vinther, B., Svensson, A.,  
350 Rasmussen, S.O., Severi, M., Blunier, T., Leuenberger, M., Fischer, H., Masson-Delmotte, V.,  
351 Chappellaz, J. and Wolff, E.: An optimized multi-proxy, multi-site Antarctic ice and gas orbital  
352 chronology (AICC2012): 120-800 ka, *Clim. Past*, 9(4), 1715–1731, 2013
- 353 Bonne, J.-L., H. C. Steen-Larsen, C. Risi, M. Werner, H. Sodemann, J.-L. Lacour, X. Fettweis, G. Cesana,  
354 M. Delmotte, O. Cattani, P. Vallelonga, H. A. Kjaer, C. Clerbaux, A. E. Sveinbjornsdottir and V. Masson-  
355 Delmotte: The summer 2012 Greenland heat wave: In situ and remote sensing observations of water  
356 vapor isotopic composition during an atmospheric river event; *Journal of Geophysical Research-  
357 Atmospheres*, 120(7), 2970-2989, 2015
- 358 Boyle, E. A.: Cool tropical temperatures shift the global  $\delta^{18}\text{O-T}$  relationship: An explanation for the  
359 ice core  $\delta^{18}\text{O}$ -borehole thermometry conflict?, *Geophysical Research Letters*, 24(3), 273-276, 1994
- 360 Broecker, W. and Putnam, A.E.: How did the hydrologic cycle respond to the two-phase mystery  
361 interval?, *Quat. Sci. Rev.*, 57(C), 17–2, 2012
- 362 Buiron, D., Stenni, B., Chappellaz, J., Landais, A., Baumgartner, M., Bonazza, M., Capron, E., Frezzotti,  
363 M., Kageyama, M., Lemieux-Dudon, B., Masson-Delmotte, V., Parrenin, F., Schilt, A., Selmo, E., Severi,  
364 M., Swingedouw, D. and Udisti, R.: Regional imprints of millennial variability during the MIS 3 period  
365 around Antarctica, *Quat. Sci. Rev.*, 48, 99-112, 2012
- 366 Buizert, C., Gkinis, V., Severinghaus, J.P., He, F., Lecavalier, B. S., Kindler, P., Leuenberger, M., Carlson,  
367 A.E., Vinther, B., Masson-Delmotte, V., White, J.W.C., Liu, Z., Otto-Bliesner and B., Brook, E.J.:  
368 Greenland temperature response to climate forcing during the last deglaciation, *Science*, 345(6201),  
369 1177–1180, 2014
- 370 Chiang, J. C. H. and Bitz, C.M.: Influence of high latitude ice cover on the marine Intertropical  
371 Convergence Zone, *Clim. Dyn.*, 25(5), 477–496, 2005
- 372 Clark, P.U., Shakun, J.D., Baker, P.A., Bartlein, P.J., Brewer, S., Brook, E., Carlson, A.E., Cheng, H.,  
373 Kaufman, D.S., Liu, Z., Marchitto, T.M., Mix, A.C., Morrill, C., Otto-bliesner, B.L., Pahnke, K., Russell,  
374 J.M., Whitlock, C., Adkins, J.F., Blois, J.L., Clark, J., Colman, S. M., Curry, W. B., Flower, B. P., He, F.,  
375 Johnson, T.C., Lynch-Stieglitz, J., Markgraf, V., Mcmanus, J., Mitrovica, J.X., Moreno, P.I. and Williams,  
376 J.W.: Global climate evolution during the last deglaciation, *PNAS*, 109(19), E1134-E1142, 2012
- 377 Dahl-Jensen, D., Mosegaard, K., Gundestrup, N., Clow, G.D., Johnsen, S.J., Hansen, A.W. and Balling,  
378 N.: Past Temperatures Directly from the Greenland Ice Sheet, *Science*, 282(5387), 268–271, 1998
- 379 Dansgaard, W.: Stable isotopes in precipitation, *Tellus*, 16, 436–468, 1964
- 380 Denton, G. H., Broecker, W.S. and Alley, R.B.: The mystery interval 17.5 to 14.5 kyrs ago PAGES news,  
381 14(20), 14–16, 2006
- 382 Denton, G.H., Anderson, R.F., Toggweiler, J.R., Edwards, R.L., Schaefer, J.M. and Putnam, A.E.: The  
383 Last Glacial Termination, *Science*, 328, 1652–1656, 2010
- 384 Epica community members: One-to-one coupling of glacial climate variability in Greenland and  
385 Antarctica, *Nature*, 444(7116), 195–198, 2006



- 386 Epstein, S., Buchsbaum, R., Lowenstam, H.A. and Urey, H.: Revised carbonate-water isotopic  
387 temperature scale GSA bulletin, 64(11), 1315-1325, 1953
- 388 Gherardi, J.-M., Labeyrie, L., McManus, J.F., Francois, R., Skinner, L.C. and Cortijo, E.: Evidence from  
389 the Northeastern Atlantic basin for variability in the rate of the meridional overturning circulation  
390 through the last deglaciation, *Earth Planet. Sci. Lett.*, 240(3), 710–723, 2005
- 391 Grootes, P. M., Stuiver, M., White, J. W. C., Johnsen, S. and Jouzel, J.: Comparison of oxygen isotope  
392 records from the GISP2 and GRIP Greenland ice cores, *Nature*, 366, 552–554, 1993
- 393 Grousset, F.: Les changements abrupts du climat depuis 60 000 ans / Abrupt climatic changes over  
394 the last 60,000 years, *Quaternaire*, 12(4), 203–211, 2001
- 395 Guillevic, M., Bazin, L., Landais, A., Stowasser, C., Masson-Delmotte, V., Blunier, T., Eynaud, F.,  
396 Falourd, S., Michel, E., Minster, B., Popp, T., Prié, F. and Vinther, B. M.: Evidence for a three-phase  
397 sequence during Heinrich Stadial 4 using a multiproxy approach based on Greenland ice core records,  
398 *Clim. Past*, 10, 2115-2133, 2014
- 399 Hillaire-Marcel, C. and De Vernal, A.: Stable isotope clue to episodic sea ice formation in the glacial  
400 North Atlantic, *Earth Plan. Sci. Lett.*, 268, 143–150, 2008
- 401 Hodell, D.A., Nicholl, J.A., Bontognali, T.R.R., Danino, S., Dorador, J., Dowdeswell, J.A., Einsle, J.,  
402 Kuhlmann, H., Martrat, B., Mleneck-vautraviers, M.J., Rodríguez-tovar, F.J. and Röhl, U.: Anatomy of  
403 Heinrich Layer 1 and its role in the last deglaciation, *Paleoceanography and Paleoclimatology*, 32(3),  
404 10.1002/2016PA003028, 2017
- 405 Johnsen, S. J., Dansgaard, W. and White, J.W.C.: The origin of Arctic precipitation under present and  
406 glacial conditions, *Tellus B*, 41B(4), 452–468, 1989
- 407 Jones, T. R., Roberts, W. H. G., Steig, E.J., Cuffey, K.M., Markle, B.R. and White, J.W.C.: Southern  
408 Hemisphere climate variability forced by Northern Hemisphere ice-sheet topography, *Nature*, 554,  
409 351-355, 2018
- 410 Jouzel, J., Merlivat, L. and Lorius, C.: Deuterium excess in an East Antarctic ice core suggests higher  
411 relative humidity at the oceanic surface during the last glacial maximum, *Nature*, 299, 688-691, 1982
- 412 Jouzel, J., Masson-Delmotte, V., Stiévenard, M. and Landais, A.: Rapid deuterium-excess changes in  
413 Greenland ice cores : a link between the ocean and the atmosphere, *Comptes Rendus - Geosci.*, 337,  
414 957–969, 2005
- 415 Kindler, P., Guillevic, M., Baumgartner, M., Schwander, J., Landais, A. and Leuenberger, M.:  
416 Temperature reconstruction from 10 to 120 kyr b2k from the NGRIP ice core, *Clim. Past*, 10(2), 887–  
417 902, 2014
- 418 Klein, E.S., Cherry, J.E., Young, J., Noone, D., Leffler, A.J. and Welker, J.M.: Arctic cyclone water vapor  
419 isotopes support past sea ice retreat recorded in Greenland ice Sci. Rep.5: 10295-10300, 2015
- 420 Kopec, B.G., Feng, X., Michel, F.A. and Posmentier, E.S., Influence of sea ice on Arctic precipitation  
421 *Proc. Natl. Acad. Sci.*, 113(1), 46–51, 2016
- 422 Krinner, G., Genthon, C. and Jouzel, J.: GCM analysis of local influences on ice core  $\delta$  signals.  
423 *Geophysical Research Letters*, 24(22), 2825-2828, 1997
- 424 Landais, A., Barkan, E. and Luz, B.: Record of  $\delta^{18}\text{O}$  and  $^{17}\text{O}$ -excess in ice from Vostok Antarctica during  
425 the last 150,000 years, *Geophys. Res. Lett.* 35(2): L02709, 2008



- 426 Landais, A., Steen-Larsen, H.C., Guillevic, M., Masson-Delmotte, V., Vinther and B., Winkler, R.: Triple  
427 isotopic composition of oxygen in surface snow and water vapor at NEEM (Greenland) *Geochim.*  
428 *Cosmochim. Acta*, 77, 304–316, 2012
- 429 Langen, P.L. and Vinther, B.M.: Response in atmospheric circulation and sources of Greenland  
430 precipitation to glacial boundary conditions, *Clim. Dyn.*, 32(7–8), 1035–1054, 2009
- 431 Leng W, von Dobeneck T, Bergmann F, Just J., Mulitza S., Chiessi C., St-Onge G. and Piper D.:  
432 Sedimentary and rock magnetic signatures and event scenarios of deglacial outburst floods from the  
433 Laurentian Channel Ice Stream, *Quat Sci Rev.*, 186, 27–46,  
434 doi:<https://doi.org/10.1016/j.quascirev.2018.01.016>, 2018
- 435 Marcott, S. A, Bauska, T.K., Buizert, C., Steig, E.J., Rosen, J.L., Cuffey, K.M., Fudge, T.J., Severinghaus,  
436 J.P., Ahn, J., Kalk, M.L., McConnell, J.R., Sowers, T., Taylor, K. C., White, J.W.C. and Brook, E.J.:  
437 Centennial-scale changes in the global carbon cycle during the last deglaciation, *Nature*, 514(7524),  
438 616–619, 2013
- 439 Markle, B.R., Steig, E. J., Buizert, C., Schoenemann, S. W., Bitz, C. M., Fudge, T. J., Pedro, J. B., Ding,  
440 Q., Jones, T.R., White, J.W.C. and Sowers, T.: Global atmospheric teleconnections during Dansgaard–  
441 Oeschger events, *Nat. Geosci.* 10(1), 36–40, 2016
- 442 Martrat, B., Jimenez-Amat, P., Zahn, R. and Grimalt, J.O.: Similarities and dissimilarities between the  
443 last two deglaciations and interglaciations in the North Atlantic region, *Quat. Sci. Rev.*, 99, 122–134,  
444 2014
- 445 Masson-Delmotte, V., Landais, A., Stievenard, M., Cattani, O., Falourd, S., Jouzel, J., Johnsen, S. J.  
446 Dahl-Jensen, D., Sveinbjornsdottir, A., White, J.W.C., Popp, T. and Fischer, H., Holocene climatic  
447 changes in Greenland: Different deuterium excess signals at Greenland Ice Core Project (GRIP) and  
448 NorthGRIP, *J. Geophys. Res. D Atmos.*, 110(14), 1–13, 2005a
- 449 Masson-Delmotte, V., Jouzel, J., Landais, A., Stievenard, M., Johnsen, S.J., White, J.W.C., Werner, M.,  
450 Sveinbjornsdottir, A. and Fuhrer, K.: GRIP deuterium excess reveals rapid and orbital-scale changes in  
451 Greenland moisture origin, *Science*, 309(5731), 118–121, 2005b
- 452 McManus, J. F., Francois, R., Gherardi, J.-M., Keigwin, L.D. and Brown-Leger S.: Collapse and rapid  
453 resumption of Atlantic meridional circulation linked to deglacial climate changes, *Nature*, 428(6985),  
454 834–837, 2004
- 455 NGRIP community members, High-resolution climate record of Northern Hemisphere climate  
456 extending into the last interglacial period, *Nature*, 431, 147–151, 2004
- 457 Partin, J. W., Cobb, K. M., Adkins, J. F., Clark, B. and Fernandez, D. P.: Millennial scale trends in west  
458 Pacific warm pool hydrology since the Last Glacial Maximum, *Nature*, 449, 452–455, 2007.
- 459 Peck, V. L., Hall, I.R., Zahn, R., Elderfield, H. and Grousset, F.: High resolution evidence for linkages  
460 between NW European ice sheet instability and Atlantic Meridional Overturning Circulation, *Earth*  
461 *Plan. Sci. Let.*, 243, 476–488, 2006
- 462 Pfahl, S. and Sodemann, H.: What controls deuterium excess in global precipitation?, *Clim. Past* 10(2),  
463 771–781, 2014
- 464 Rasmussen, S.O., Andersen, K.K., Svensson, A.M., Steffensen, J.P., Vinther, B.M., Clausen, H.B.,  
465 Siggaard-Andersen, M.L., Johnsen, S.J., Larsen, L.B., Dahl-Jensen, D., Bigler, M., Roethlisberger, R.,



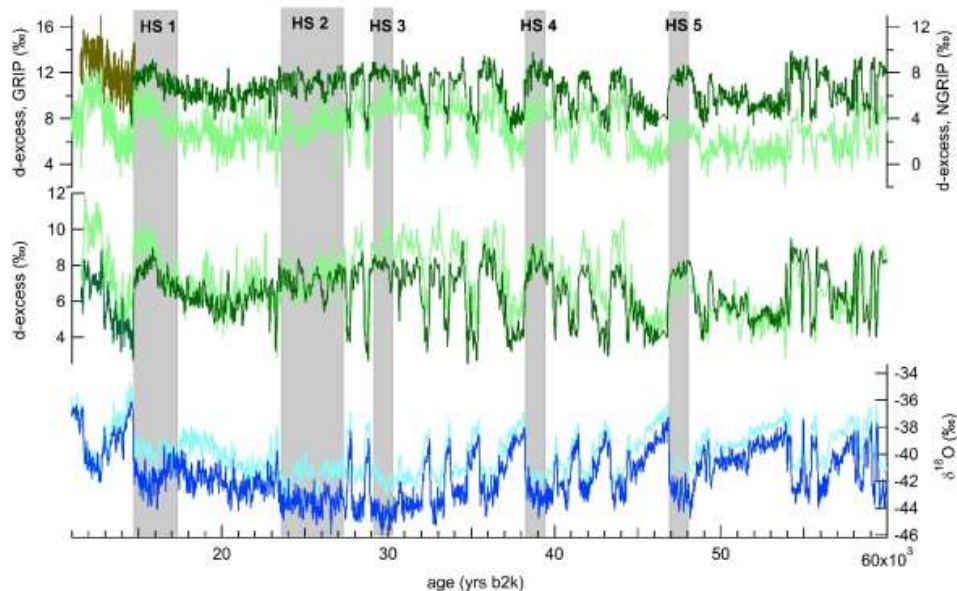
- 466 Fischer, H., Goto-Azuma, K., Hansson, M.E. and Ruth, U.: A new Greenland ice core chronology for  
467 the last glacial termination, *J. Geophys. Res. Atmos.*, 111(6), 1–16, 2006
- 468 Rasmussen, S.O., Seierstad, I.K., Andersen, K.K., Bigler, M. and Johnsen, S.J.: Synchronization of the  
469 NGRIP, GRIP, and GISP2 ice cores across MIS 2 and palaeoclimatic implications, *Quat. Sci. Res.*, 27,  
470 18–28, 2008
- 471 Rhines, A. and Huybers, P.J.: Sea ice and dynamical controls on preindustrial and last glacial  
472 maximum accumulation in central Greenland *J. Clim.* 27(23): 8902–8917, 2014
- 473 Rhodes, R.H., Brook, E.J., Chiang, J. C. H., Blunier, T., Maselli, O.J., McConnell, J., Romanini, D. and  
474 Severinghaus, J.P.: Enhanced tropical methane production in response to iceberg discharge in the  
475 North Atlantic, *Science*, 348(6238), 1016–1019, 2015
- 476 Risi, C., Landais, A., Bony, S., Jouzel, J., Masson-Delmotte, V. and Vimeux, F.: Understanding the  $^{17}\text{O}$   
477 excess glacial-interglacial variations in Vostok precipitation, *J. Geophys. Res. Atmos.*, 115(10),  
478 D10112, 2010
- 479 Russell, J., Vogel, H., Konecky, B.L., Bijaksana, S., Huang, Y., Melles, M., Wattrus, N., Costa, K. and  
480 King, J.W.: Glacial forcing of central Indonesian hydroclimate since 60,000 y BP., *Proc. Natl Acad. Sci.*,  
481 111, 5100–5105, 2014
- 482 Schoenemann, S. W., Schauer, S. and Steig, E.J.: Measurement of SLAP2 and GISP d17O and proposed  
483 VSMOW-SLAP normalization for d17O and  $^{17}\text{O}$ excess, *Rapid Commun. Mass Spectrom.*, 27(5), 582–  
484 590, 2013
- 485 Schoenemann, S.W., Steig, E.J., Ding, Q., Markle, B.R. and Schauer, A.J.: Triple water-isotopologue  
486 record from WAIS Divide, Antarctica: Controls on glacial-interglacial changes in  $^{17}\text{O}$ -excess of  
487 precipitation, *J. Geophys. Res. Atmos.*, 119(14), 8741–8763, 2014
- 488 Schoenemann, S.W. and Steig, E.J.: Seasonal and spatial variations of  $^{17}\text{O}$ -excess and d-excess in  
489 Antarctic precipitation: Insights from an intermediate complexity isotope model, *J. Geophys. Res.*  
490 *Atmos.*, 121(19), 11,211–215,247, 2016
- 491 Severinghaus, J. P. and Brook, E.: Abrupt climate change at the end of the last glacial period inferred  
492 from trapped air in polar ice, *Science*, 286 (5441), 930–934, 1999
- 493 Stanford, D., Rohling, E. J., Bacon, S., Roberts, A.P., Grousset, F.E. and Bolshaw, M.: A new concept for  
494 the paleoceanographic evolution of Heinrich event 1 in the North Atlantic, *Quat. Sci. Rev.*, 30(9–10),  
495 1047–1066, 2011
- 496 Steffensen, J. P., Andersen, K.K., Bigler, M., Clausen, H.B., Dahl-Jensen, D., Fischer, H., Goto-Azuma,  
497 K., Hansson, M., Johnsen, S.J., Jouzel, J., Masson-Delmotte, V., Popp, T., Rasmussen, S.O.,  
498 Rothlisberger, R., Ruth, U., Stauffer, B., Siggaard-Andersen, M.-L., Sveinbjörnsdóttir, A. E., Svensson,  
499 A. and White, J.W.C., High-Resolution Greenland Ice Core Data Show Abrupt Climate Change  
500 Happens in Few Years *Science*, 321(5889), 680–684, 2008
- 501 Stenni, B., Buiron, D., Frezzotti, M., Albani, S., Barbante, C., Bard, E., Barnola, J.M., Baroni, M.,  
502 Baumgartner, M., Bonazza, M., Capron, E., Castellano, E., Chappellaz, J., Delmonte, B., Falourd, S.,  
503 Genoni, L., Iacumin, P., Jouzel, J., Kipfstuhl, S., Landais, A., Lemieux-Dudon, B., Maggi, V., Masson-  
504 Delmotte, V., Mazzola, C., Minster, B., Montagnat, M., Mulvaney, R., Narcisi, B., Oerter, H., Parrenin,  
505 F., Petit, J.R., Ritz, C., Scarchilli, C., Schilt, A., Schüpbach, S., Schwander, J., Selmo, E., Severi, M.,



- 506 Stocker, T.F. and Udisti, R.: Expression of the bipolar see-saw in Antarctic climate records during the  
507 last deglaciation, *Nat. Geosci.*, 4(1), 46-49, 2011
- 508 Stríkis, N.M., Chiessi, C.M., Cruz, F.W., Vuille, M., Cheng, H., De Souza Barreto, E.A., Mollenhauer, G.,  
509 Kasten, S., Karmann, I., Edwards, R.L., Bernal, J.P. and Sales, H.D.R.: Timing and structure of Mega-  
510 SACZ events during Heinrich Stadial 1, *Geophys. Res. Lett.*, 42 (13), 5477–5484, 2015.
- 511 Svensson, A., Andersen, K.K., Bigler, M., Clausen, H.B., Dahl-Jensen, D., Davies, S.M., Johnsen, S.J.,  
512 Muscheler, R., Parrenin, F., Rasmussen, S.O., Röthlisberger, R., Seierstad, I., Steffensen, J.P. and  
513 Vinther, B.M.: A 60 000 year Greenland stratigraphic ice core chronology, *Clim. Past*, 4 (1), 47–57,  
514 2008
- 515 Toucanne, S., Zaragosi, S., Bourillet, J.-F., Marieu, V., Cremer, M., Kageyama, M., Van Vliet-Lanoë, B.,  
516 Eynaud, F., Turon, J.-L. and Gibbard, P.-L.: The first estimation of Fleuve Manche palaeoriver  
517 discharge during the last deglaciation: Evidence for Fennoscandian ice sheet meltwater flow in the  
518 English Channel ca 20-18 ka ago, *Earth Planet. Sci. Lett.*, 290(3–4), 459–473, 2010
- 519 Toucanne, S., Soulet, G., Freslon, N., Silva Jacinto, R., Dennielou, B., Zaragosi, S., Eynaud, F., Bourillet,  
520 J.-F. and Bayon, G.: Millennial-scale fluctuations of the European Ice Sheet at the end of the last  
521 glacial, and their potential impact on global climate, *Quaternary Science Reviews*, 123, 113-133, 2015
- 522 Touzeau, A., Landais, A., Stenni, B., Uemura, R., Fukui, K., Fujita, S., Guilbaud, S., Ekaykin, A., Casado,  
523 M., Barkan, E., Luz, B., Magand, O., Teste, G., Le Meur, E., Baroni, M., Savarino, J., Bourgeois, I. and  
524 Risi, C.: Acquisition of isotopic composition for surface snow in East Antarctica and the links to  
525 climatic parameters, *The Cryosphere*, 10, 837–852, 2016
- 526 Uemura, R., Masson-Delmotte, V., Jouzel, J., Landais, A., Motoyama, H. and Stenni, B.: Ranges of  
527 moisture-source temperature estimated from Antarctic ice cores stable isotope records over glacial–  
528 interglacial cycles, *Clim. Past* 8(3), 1109–1125, 2012
- 529 Ullman, D.J., Carlson, A.E., Anslow, F.S., LeGrande, A.N. and Licciardi, J.M.: Laurentide ice-sheet  
530 instability during the last deglaciation, *Nat. Geosci.*, 8(7), 534-537, 2015
- 531 Vaughn, B., H., White, J.W.C., Delmotte, M., Trolier, M., Cattani, O. and Stievenard, M.: An  
532 automated system for hydrogen isotope analysis of water, *Chemical Geology Including Isotope*  
533 *Geoscience*, 152, 309-319, 1998
- 534 Veres, D., Bazin, L., Landais, A., Toyé Mahamadou Kele, H., Lemieux-Dudon, B., Parrenin, P.,  
535 Martinerie, P., Blayo, E., Blunier, T., Capron, E., Chappellaz, J., Rasmussen, S.O., Severi, M., Svensson,  
536 A., Vinther, B. and Wolff, E.W., The Antarctic ice core chronology (AICC2012): an optimized multi-  
537 parameter and multi-site dating approach for the last 120 thousand years, *Clim. Past*, 9(4), 1733–  
538 1748, 2013
- 539 Wais Divide Members: Onset of deglacial warming in West Antarctica driven by local orbital forcing  
540 *Nature*, 500(7463), 440–444, 2013
- 541 Winkler, R., Landais, A., Sodemann, H., Dümbgen, L., Prié, F., Masson-Delmotte, V., Stenni, B. and  
542 Jouzel, J.: Deglaciation records of <sup>17</sup>O-excess in East Antarctica: Reliable reconstruction of oceanic  
543 normalized relative humidity from coastal sites, *Clim. Past*, 8(1), 1–16, 2012
- 544 Zhang, W., Wu, J., Wang, Y., Wang, Y., Cheng, H., Kong, X. and Duan, F. A: detailed East Asian  
545 monsoon history surrounding the ‘Mystery Interval’ derived from three Chinese speleothem records,  
546 *Quat. Res.*, 82(1), 154–163, 2014

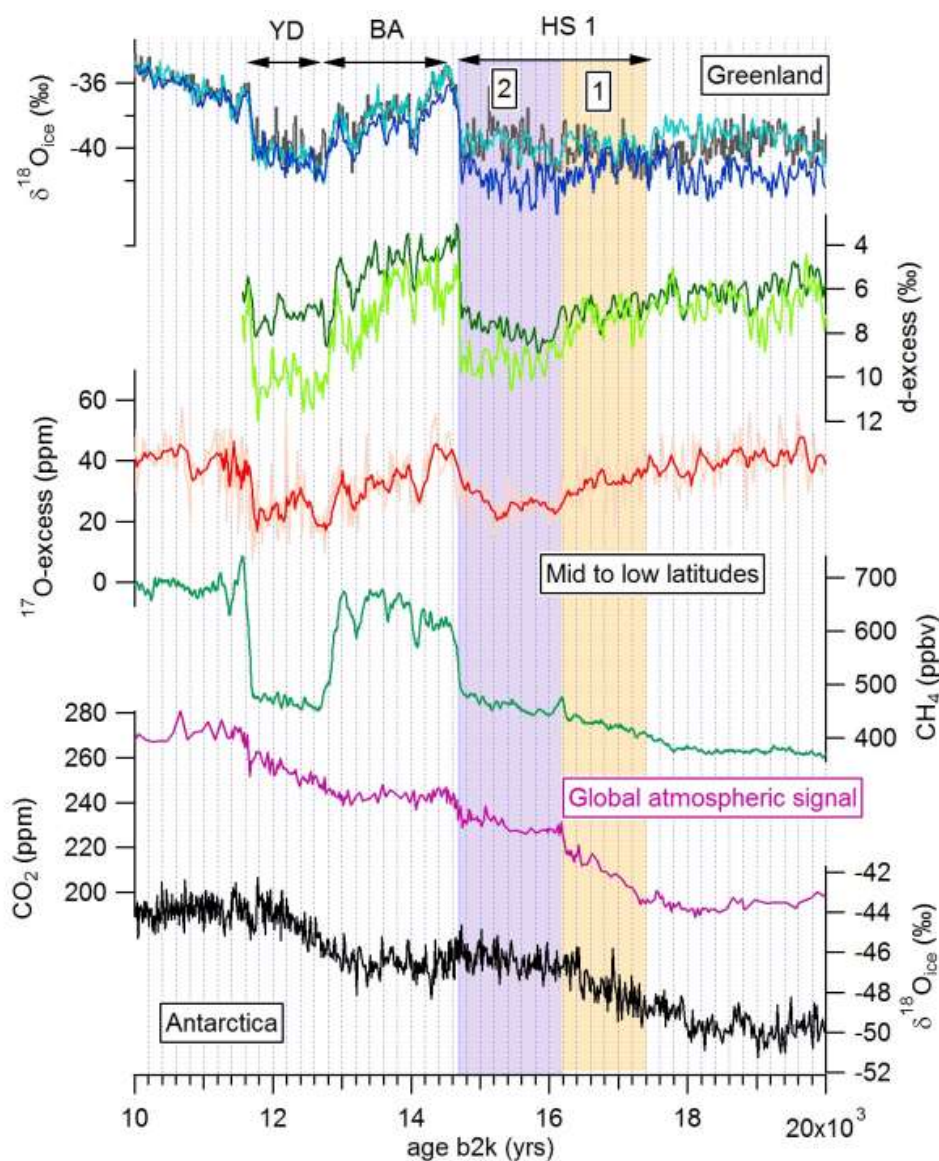


547



548

549 **Figure 1:** water stable isotope records ( $\delta^{18}\text{O}$  and  $d$ -excess, in ‰) from GRIP and NGRIP ice cores  
550 reported on the GICC05 chronology (in thousands of years before year 2000 CE). From top to bottom:  
551 -  $d$ -excess from the NGRIP ice core (khaki: data obtained at INSTAAR SIL, Steffensen et al., 2008;  
552 dark green: data obtained at LSCE, this study);  $d$ -excess from the GRIP ice core (light green,  
553 Masson-Delmotte et al., 2005)  
554 -  $d$ -excess from the NGRIP ice core after correction of the shift between INSTAAR SIL and LSCE  
555 (dark green) dataset, and  $d$ -excess from the GRIP ice core (light green).  
556 -  $\delta^{18}\text{O}$  from the NGRIP ice core (dark blue) datasets,  $\delta^{18}\text{O}$  from the GRIP ice core (light blue).  
557 Grey intervals display Heinrich Stadials (HS).  
558



559

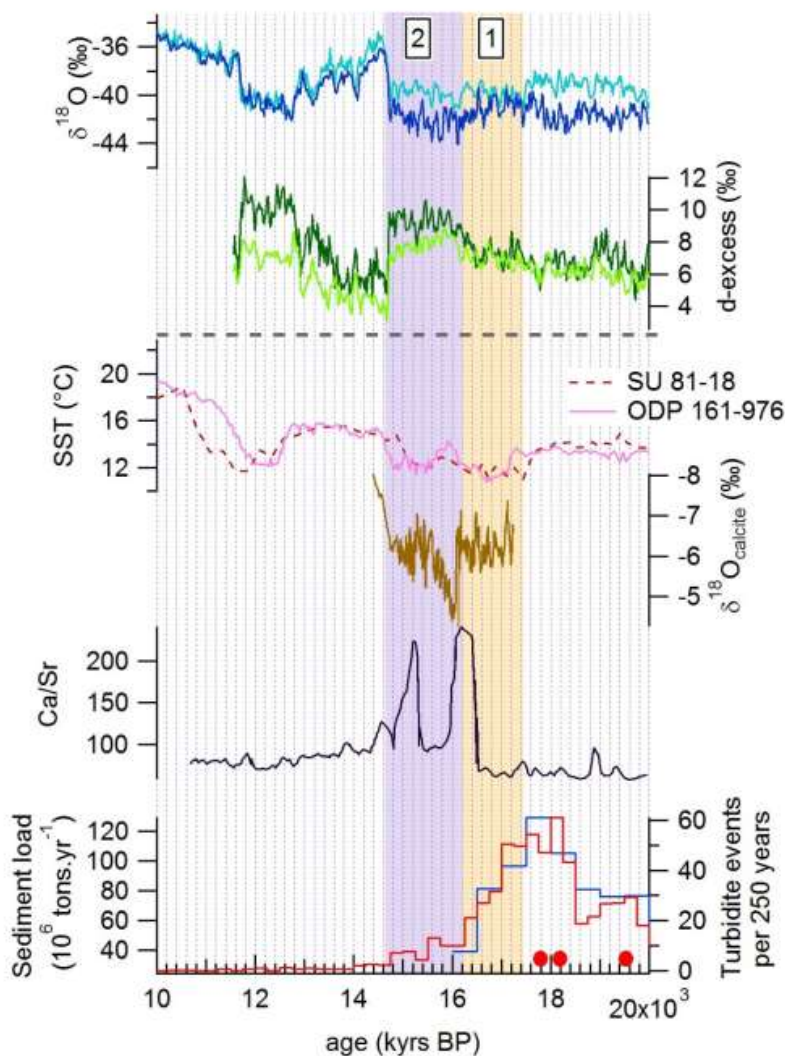
560 **Figure 2:** A synthesis of ice core records over the last deglaciation on the synchronized GICC05/AICC2012  
 561 timescales with an identification of two phases (1, orange box and 2, purple box) within Heinrich Stadial  
 562 1 (HS1) as discussed in the text: we locate the transition between phases 1 and 2 at the timing of the  
 563 sharp increase in CO<sub>2</sub> and CH<sub>4</sub> concentrations, both being global atmospheric composition signals. The  
 564 Younger Dryas (YD) and Bølling-Allerød (BA) periods are also indicated.

565 From top to bottom:

- 566 - GRIP, NGRIP and GISP2  $\delta^{18}\text{O}$  (light blue, dark blue and black respectively (Grootes et al., 1993;  
 567 NGRIP community members, 2004) interpolated at a 20 years resolution
- 568 - GRIP and NGRIP d-excess (light and dark green respectively: Jouzel et al., 2005, this study)  
 569 interpolated at a 20 years resolution



- 570 - *NGRIP <sup>17</sup>O-excess (orange curve shows the original series and the red curve the 5 years running*  
571 *average, this study)*
- 572 - *WAIS Divide CH<sub>4</sub> (Rhodes et al., 2015)*
- 573 - *WAIS Divide CO<sub>2</sub> (Marcott et al., 2013)*
- 574 - *EPICA Dronning Maud Land (EDML) δ<sup>18</sup>O<sub>ice</sub> (EPICA community members, 2006)*
- 575



576

577 **Figure 3:** The sequence of Phase 1 and Phase 2 of Heinrich Stadial 1 identified in Greenland records  
 578 and in proxy records of North Atlantic SST, IRD events, and changes in East Asian hydroclimate. From  
 579 top to bottom:

- 580 - NGRIP (dark blue) and GRIP (light blue)  $\delta^{18}\text{O}$  records
- 581 - NGRIP (dark green) and GRIP (light green) d-excess records
- 582 - Sea surface temperature (SST) for North Atlantic cores SU 81-18 (Bard et al., 2000) and ODP
- 583 161-976 (Martrat et al., 2014).
- 584 - Calcite  $\delta^{18}\text{O}$  of Hulu cave (China, Zhang et al., 2014)
- 585 - Ca/Sr from site U1308 in the IRD belt (Hodell et al., 2019) as signature from strong iceberg
- 586 discharges from the Laurentide ice sheet.
- 587 - Indications for Channel River sediment load (blue, sediment load; red, turbidite frequency)
- 588 (Toucanne et al., 2010; 2015) as signature for meltwater input from European side. The 3 red
- 589 circles indicate plumite layers resulting from outburst floods on the Eastern Canadian margin



590                    *(Leng et al., 2018), i.e. meltwater arrival from the North America side in the absence of strong*  
591                    *iceberg discharge.*  
592                    *The dashed horizontal line separates the ice core records on the GICC05 timescale from non ice core*  
593                    *records on their own timescales.*

594

595

596